MATHEMATICAL MODELLING
МАТЕМАТИЧЕСКОЕ МОДЕЛИРОВАНИЕ

Check for updates

Original Theoretical Research

UDC 519.6
https://doi.org/10.23947/2587-8999-2024-8-2-45-49

# Modelling of Capillary Discharge in Repetition Mode for Short Capillary Systems with Various Filling Methods

**Vladimir A. Gasilov, Nikita O. Savenko ✉, Yulia S. Sharova**
Keldysh Institute of Applied Mathematics of Russian Academy of Sciences, Moscow, Russian Federation
✉savenkonkt@gmail.com

**Abstract**
***Introduction.*** Currently, frequency modes of operation of electron accelerators based on capillary discharges are actively investigated. Electrons in these systems are accelerated by femtosecond laser pulses passing through the discharge plasma.
***Materials and Methods.*** The paper presents results of three-dimensional magnetohydrodynamic modelling of the capillary discharge cycle, including stages of filling a short capillary with working gas (hydrogen), formation of the plasma channel, and restoration of the working medium before the start of the next discharge. Calculations were performed assuming the system is under external cooling, which maintains thermal balance at intermediate stages of the working cycle, and under constant conditions of gas supply and evacuation.
***Results.*** The computational experiments demonstrate the capability of generating beams of relativistic electrons with a repetition frequency of approximately one kilohertz.
***Discussion and Conclusions.*** The obtained results allow us to speak about the prospects of using LWFA with a short channel length and a high repetition rate of the capillary discharge.

**Keywords:** mathematical modelling, magnetohydrodynamics, capillary discharge, laser acceleration of electrons

**Acknowledgements.** The results were obtained using the equipment of the “Center for Collective Use” IAM RAS (ckp.kiam.ru). The authors are grateful to candidate of physical and mathematical sciences G.A. Bagdasarov for discussing the results of computational experiments.

**For citation.** Gasilov V.A., Savenko N.O., Sharova Yu.S. Modelling of capillary discharge in repetition mode for short capillary systems with different filling methods. *Computational Mathematics and Information Technologies*. 2024;8(2):45–59. https://doi.org/10.23947/2587-8999-2024-8-2-45-59

*Оригинальное теоретическое исследование*

# Моделирование капиллярного разряда в режиме повторения для коротких капиллярных систем при различных способах заполнения

**В.А. Гасилов, Н.О. Савенко ✉, Ю.С. Шарова**
Институт прикладной математики им. М.В. Келдыша Российской академии наук, г. Москва, Российская Федерация
✉savenkonkt@gmail.com

**Аннотация**
***Введение.*** В настоящее время активно исследуются частотные режимы работы ускорителей электронов на основе капиллярных разрядов. Электроны в них ускоряются под действием лазерных импульсов фемтосекундного диапазона длительности, пропускаемых через плазму разряда.
***Материалы и методы.*** В работе рассматриваются результаты трехмерного магнитогидродинамического моделирования цикла капиллярного разряда, включающего стадии заполнения короткого капилляра рабочим газом (водород), формирование плазменного канала, восстановление рабочей среды перед началом следующего разряда. Расчеты выполнены в предположении о том, что система находится под внешним охлаждением, которое

обеспечивает температурный баланс на промежуточных этапах рабочего цикла, а также при постоянных условиях подачи и откачки рабочего газа.

***Результаты исследования.*** Результаты вычислительных экспериментов показывают возможность генерации пучков релятивистских электронов с частотой повторения около одного килогерца.

***Обсуждение и заключение.*** Полученные результаты позволяют говорить о перспективности использования КЛПУ с малой длиной канала и высокой частотой повторения капиллярного разряда.

**Ключевые слова:** математическое моделирование, магнитная гидродинамика, капиллярный разряд, лазерное ускорение электронов

**Благодарности.** Результаты получены с использованием оборудования ЦКП ИПМ им. М.В. Келдыша РАН (http://ckp-kiam.ru). Авторы признательны кандидату физ.-мат. наук Г.А. Багдасарову за обсуждение результатов вычислительных экспериментов.

**Для цитирования.** Гасилов В.А., Савенко Н.О., Шарова Ю.С. Моделирование капиллярного разряда в режиме повторения для коротких капиллярных систем при различных способах заполнения. *Computational Mathematics and Information Technologies*. 2024;8(2):45–59. https://doi.org/10.23947/2587-8999-2024-8-2-45-59

**Introduction.** The method of generating relativistic electron beams in the field of laser radiation was proposed and substantiated in [1]. Since then, compact laser electron accelerators have found applications in a wide range of fundamental and applied research fields. Among these, developments in free electron lasers (FELs) [2], creation of Compton sources of radiation and electron-positron colliders [3, 4], and others have been highlighted. Works [5–8] have presented theories and results of several experiments on electron beam generation using the Laser Wakefield Acceleration (LWFA) mechanism.

Capillary discharges are widely employed in many experiments in the field of pulsed plasma physics as a simple and convenient tool for generating “quiet”, non-turbulent plasma with reliably controlled parameters. Capillary discharges as a means of creating plasma channels for laser electron acceleration and other applications are extensively discussed in works [7–15].

In several applications (medical-biological research, material sciences, etc.), there is a demand not for high-energy gains achieved by accelerated electrons, as demonstrated in experiment [13], but rather for a high repetition rate (of the order of and exceeding 1 kHz) of electron accelerator pulses. For instance, in [16], a discharge waveguide for LWFA using hydrogen as the working gas was discussed, achieving a repetition frequency of several kHz. Other plasma waveguides for LWFA operating at high repetition rates are described in works [17, 18]. Typically, such experiments utilize relatively short capillaries, approximately 1–3 cm in length. In this regard, several publications highlight the possibility of using short plasma channels to obtain electron beams with energies up to 1 GeV [18–23] as one of the main research outcomes.

This paper presents results from three-dimensional modeling of capillary discharge. The primary focus is on the formation process of the plasma waveguide, which can serve for electron acceleration by a laser pulse. Comparisons are made between computational results and theoretical estimates of accelerated electron energies. The main external factors affecting the capillary in our model include the gas flow into the capillary feeding channels and the plasma heat exchange with the capillary walls.

The research multifunctional code MARPLE, developed at the Institute of Applied Mathematics named after M.V. Keldysh [20], is utilized for modeling the described process.

**Materials and Methods.** Computational experiments to study the dynamics of capillary discharge plasma are conducted using a single-fluid two-temperature magnetohydrodynamic (MHD) model. This model incorporates electron-ion energy exchange, thermal conductivity of the ion and electron components of the plasma. The main system of equations solved includes [24]:

Continuity equation

$$\frac{\partial \rho}{\partial t} + \nabla(\rho \mathbf{V}) = 0,$$

momentum balance equation

$$\rho\left(\frac{\partial}{\partial t} + \mathbf{V}\cdot\nabla\right)\mathbf{V} = -\nabla\left(p_i + p_e\right) + \frac{1}{c}\mathbf{j}\times\mathbf{B},$$

$$\rho\left(\frac{\partial}{\partial t} + \mathbf{V}\cdot\nabla\right)\varepsilon_i + p_i\nabla\cdot\mathbf{V} = \nabla\left(\kappa_i \nabla T_i\right) - Q_{ie},$$

$$\rho\left(\frac{\partial}{\partial t} + \mathbf{V}\cdot\nabla\right)\varepsilon_e + p_e\nabla\cdot\mathbf{V} = \nabla\left(\kappa_e \nabla T_e\right) + \frac{\mathbf{j}^2}{\sigma} + Q_{ie} - Q_{\text{rad}},$$

Maxwell's equations (excluding displacement current)

$$\mathbf{j} = \frac{c}{4\pi}(\nabla \times \mathbf{B}), \quad \frac{\partial \mathbf{B}}{\partial t} = -c(\nabla \times \mathbf{E}), \quad \Delta \cdot \mathbf{B} = 0.$$

The main system of equations is closed by the equation of state in the form of

$$p_i = p_i\,(\rho, \varepsilon_i), p_e = p_e\,(n_e, \varepsilon_e),$$

and Ohm's law in the form of $\mathbf{E} = \frac{1}{c}(\mathbf{V} \times \mathbf{B}) + \frac{\mathbf{j}}{\sigma}$.

It is assumed that throughout the entire duration of the electric discharge, the condition of quasi-neutrality of the gas-plasma medium is maintained $n_e - Zn_i = 0$.

The operational cycle of the capillary is divided into three consecutive stages. The first stage involves filling the capillary with cold gas (hydrogen) until flow stabilization occurs. The second stage is the actual electric discharge necessary for forming the discharge channel in a fully ionized environment, where the termination of the electrical pulse is characterized by rapid recombination within the discharge plasma. In the final, third stage of the cycle, hot gas escapes from the capillary and is replaced by a fresh portion of gas from the feeding channels. The stages of filling and purging are calculated in a single-temperature approximation, as the presence of the electron component during this period is negligible.

The study considers two geometrical configurations of the system: with two and with eight feeding channels. The results of the calculations are compared with those from [21], obtained under the same conditions of capillary discharge implementation but in a simpler problem setup, considered in a highly idealized two-dimensional cylindrical ($r$, $z$) geometry. The capillary of circular cross-section is assumed to have a length of 2 cm and a diameter of 300 µm (see Fig. 1). The computational domain is structured as follows: the main capillary channel is modeled as a tube with open ends, to which the feeding channels of the same diameter as the capillary (300 µm) are attached at a distance of 0.8 cm from the center of the main tube. Electrodes with a half-aperture angle of 45° and a length of 0.2 cm are positioned at the ends of the capillary, followed by a free gas exit area with a length of 0.2 cm.

The construction of the computational domain for the capillary with eight feeding channels is carried out by assuming that the number of feeding channels per half-length of the capillary is four, cross-attached to the capillary. This geometry of the entire structure allows for a more homogeneous gas flow in the region where the feeding channels connect with the capillary.

The computational mesh is built considering the symmetry of the geometrical model of the system with eight feeding channels, thereby limiting calculations to one eighth of the entire area filled with the working substance (feeding channels and the main capillary tract). The electromagnetic field is computed for the capillary channel in a dielectric, as commonly implemented in most designs [2, 16, 21]. High-conductivity metal electrodes (copper, aluminum) are attached to the ends of the capillary in accordance with this design. Consequently, during the calculation stage of the electric discharge, boundary conditions for the equations of electrodynamics are applied from the general magnetohydrodynamic system. Gas dynamic equations are solved using standard impermeable wall conditions for the capillary walls, while at the open ends of the capillary, gas parameters are computed according to the methodology for implementing non-reflecting boundary conditions [22].

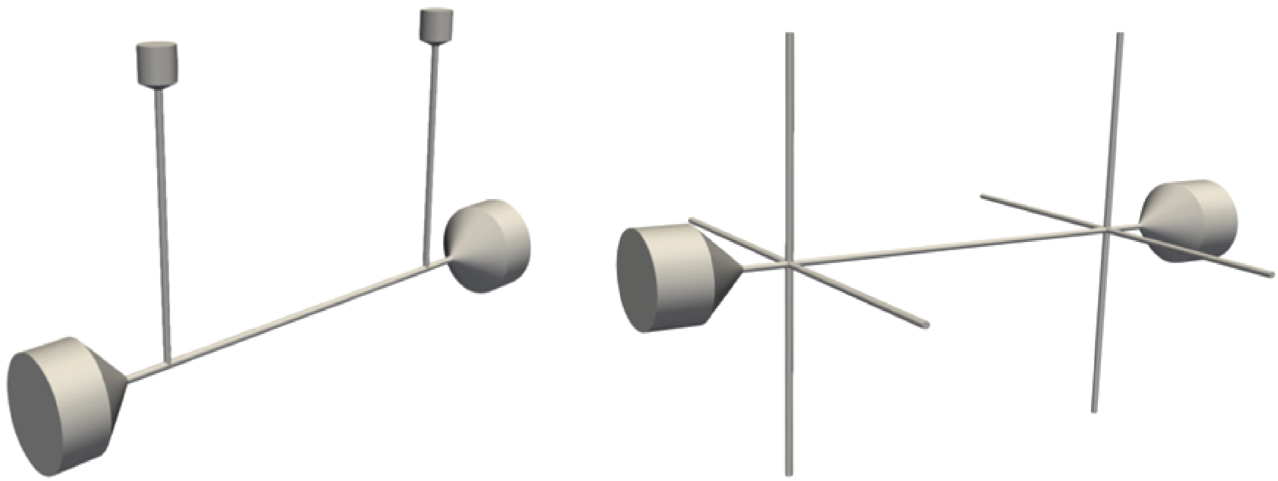

*a)* *b)*

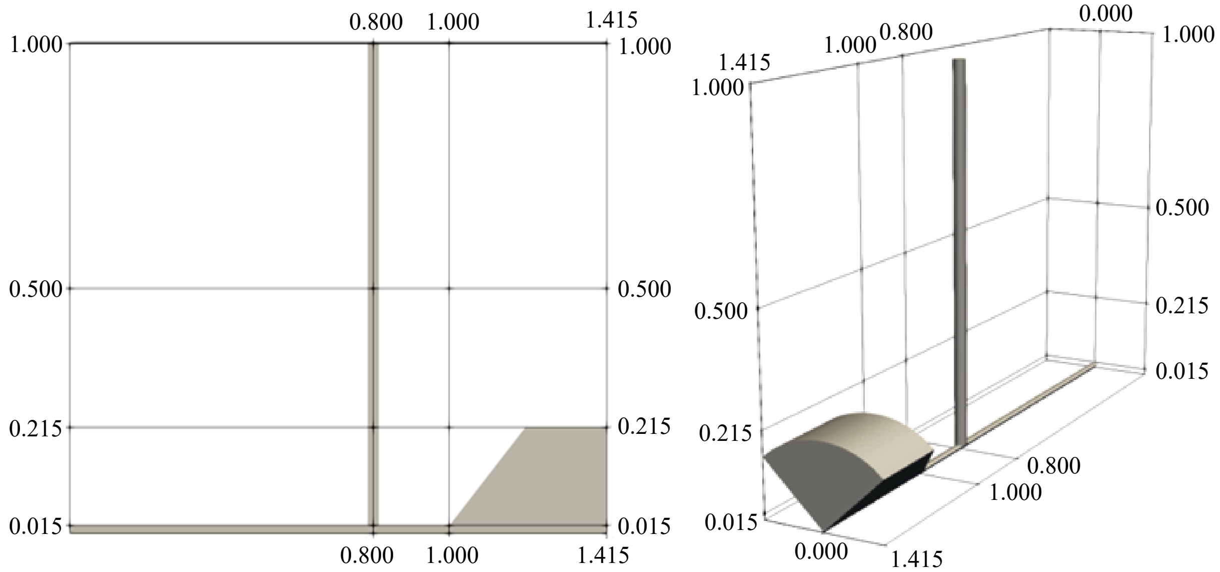


c) d)

Fig. 1. Geometry of the computational domain: *a* — general view for the system with two feeding channels; *b* — general view for the system with eight feeding channels; *c* — characteristic dimensions of the domain are identical for both considered variants of the capillary system construction; *d* — characteristic dimensions of the domain for the system with eight feeding tubes

Calculations were performed for two consecutive operating cycles. During the capillary filling stage, both primary and repeated, the inlet pressure into the feeding channels for the two-channel system was set to $p$ = 0.125 bar with a temperature of 300 K, while for the eight-channel configuration, $p \approx 0.083$ bar at 300 K was used. These inlet gas parameter values ensure equal gas flow rates during system filling and approximately equal values of gas flow parameters along the capillary axis after reaching steady-state flow conditions. Once steady-state flow is achieved within the system, the filling stage is considered complete. The gas parameters attained in the capillary at this stage serve as initial data for the discharge phase.

In accordance with numerous experiments [16–19, 21], the following dependence for the electrical current through the capillary was used for the calculations:

$$I = I_0 \frac{t}{t_{\max}} \exp\left(1 - \frac{t}{t_{\max}}\right), \qquad (1)$$

where $I_0$ = 210 A; $t$ is the current time from the start of the discharge; $t_{\max}$= 0.15 μs is the time of maximum current strength. The current pulse profile is shown in Fig. 2.

The azimuthal component of the magnetic field at the insulator boundary, specified as a boundary condition for the magnetic field, is approximately taken as $B_\varphi = 2I(t)/R$, where $I(t)$ is calculated using equation (1), and $R$ is the radius of the capillary tube. The second stage of the capillary operation concludes when the discharge current ceases. Over the subsequent short interval, the ionized substance electro-conducted recombines. The gas state during this period is assumed as the initial state for the subsequent refilling stage.

During the final stage, the process of restoring the distribution of neutral hydrogen in the capillary is simulated. This includes the expulsion of hot hydrogen from the capillary and its replacement with a new portion of cold hydrogen from the feeding channels, initiating the start of the refilling process.

For the case of eight feeding tubes, calculations for all three discharge stages are performed within one eighth of the total flow area. This is feasible due to the symmetry of the capillary construction with feeding tubes. The electrode at the end of the capillary is considered as a cylindrical layer of metal — a "ring" approximately one-tenth of the radius thick.

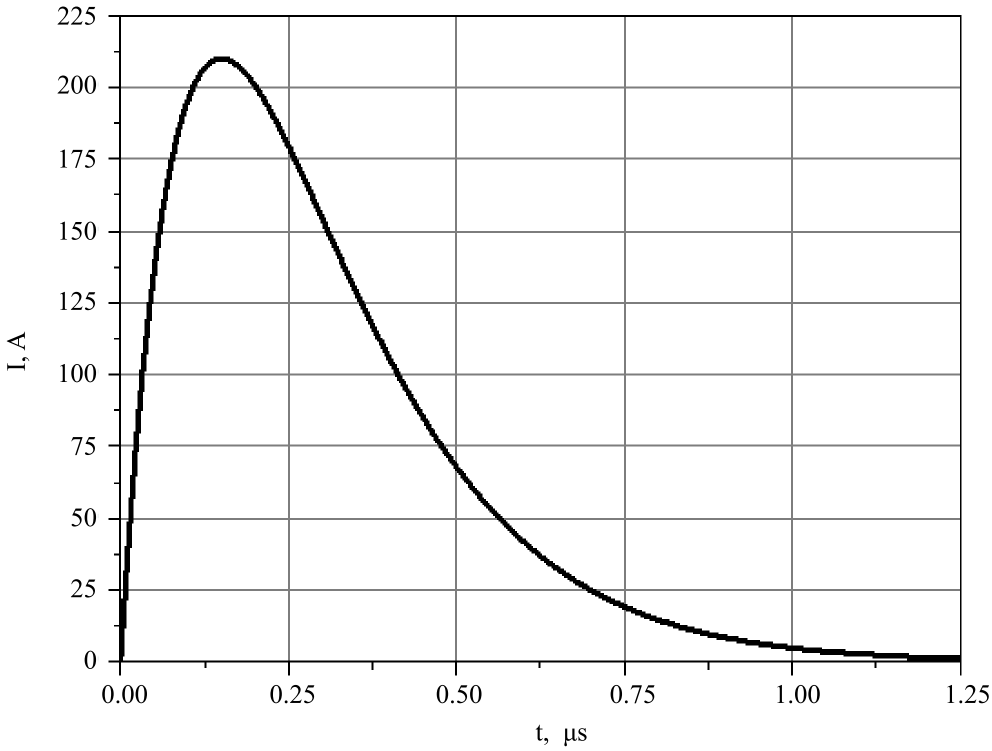


Fig. 2. Current profile as a function of time

**Results**

**Primary filling.** The primary filling stage concludes upon the establishment of steady hydrogen flow through the capillary. Fig. 3 and 4 depict density profiles along the capillary axis at various time points for systems with two and eight feeding channels (Fig. 3), as well as in the two-dimensional model (Fig. 4) with simplified (ring-shaped) gas delivery into the capillary. The corresponding stages of gas flow evolution are illustrated.

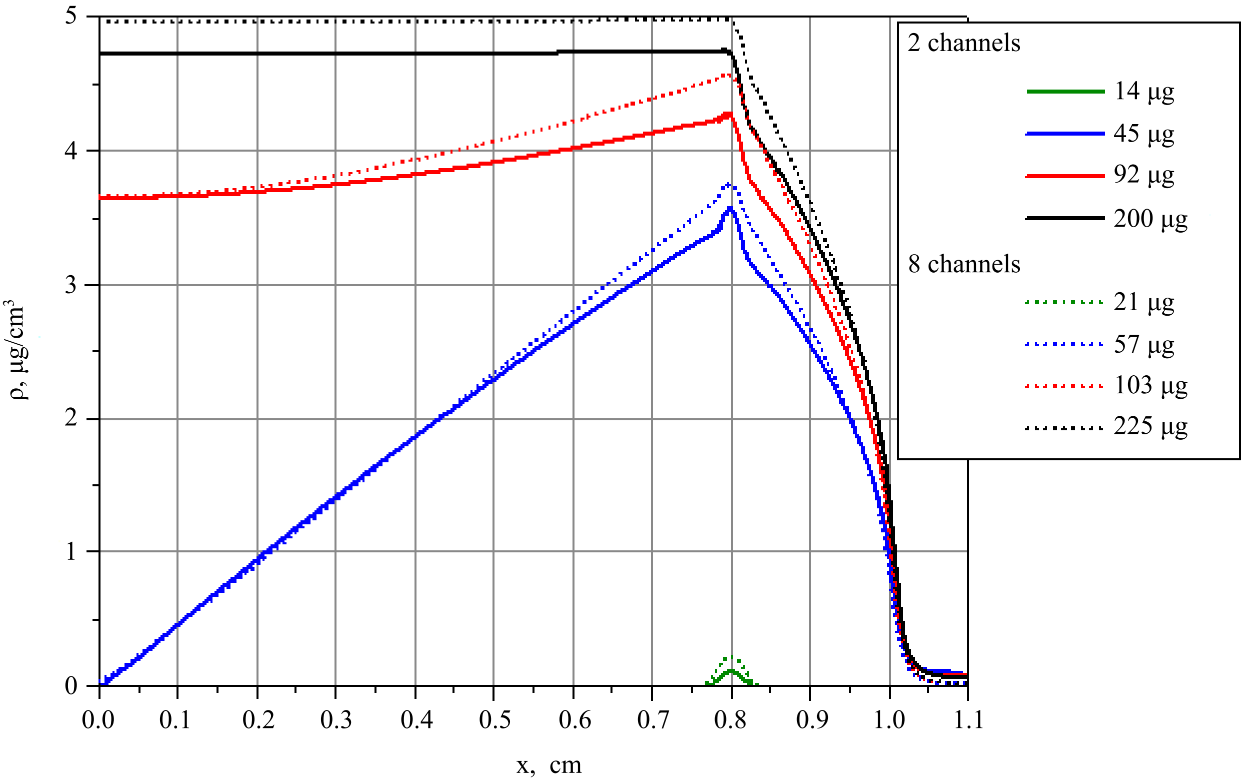


Fig. 3. Density distribution along the axis of the capillary for two geometries at corresponding time points

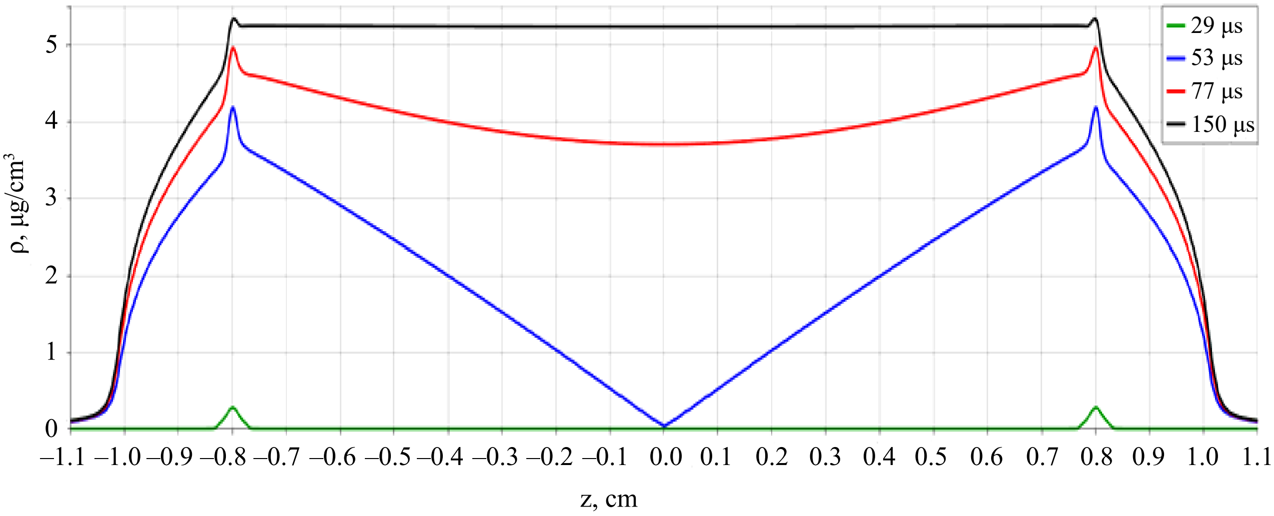


Fig. 4. Density distribution along the axis of the capillary for the two-dimensional model discussed in [21]

The slight difference in parameters upon reaching steady state does not significantly influence subsequent stages. As demonstrated in Figure 5, for three different feeding channel geometries, the establishment times are as follows: 2 feeding channels — 200 μs, 8 feeding channels — 225 μs, two-dimensional model of capillary feeding — 125 μs.

Due to thermal conductivity, the gas temperature at this stage equalizes and matches the temperature of the capillary wall, which is 300 K.

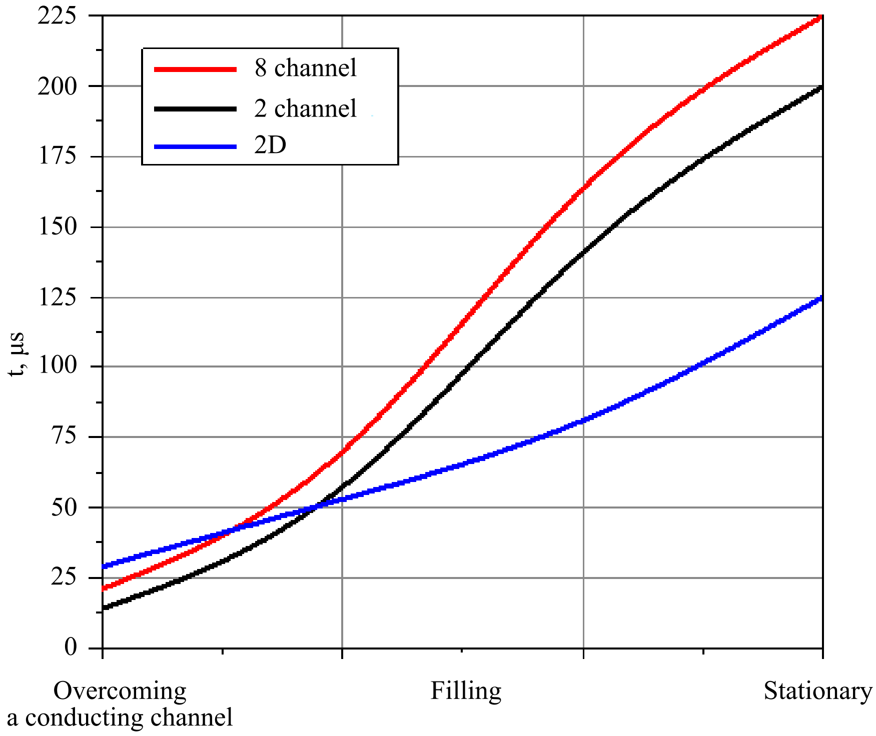


Fig. 5. Establishment time of flow during the primary filling stage for different geometries

Fig. 6 illustrates the distribution of mass flow (g/s) along the system and across the main channel near the inlet of the feeding tube (0.82 cm) for eight and two feeding tubes.

The slight yet noticeable asymmetry in flow parameters observed in different cross-sections in the case of two feeding tubes filling the capillary is indicative of the quality of the waveguide channel, which must possess sufficiently high radial symmetry to ensure the high efficiency of electron acceleration by a laser pulse. The symmetry of flow is particularly crucial in the vicinity of the capillary axis, where the channel with parameters necessary for electron acceleration is formed.

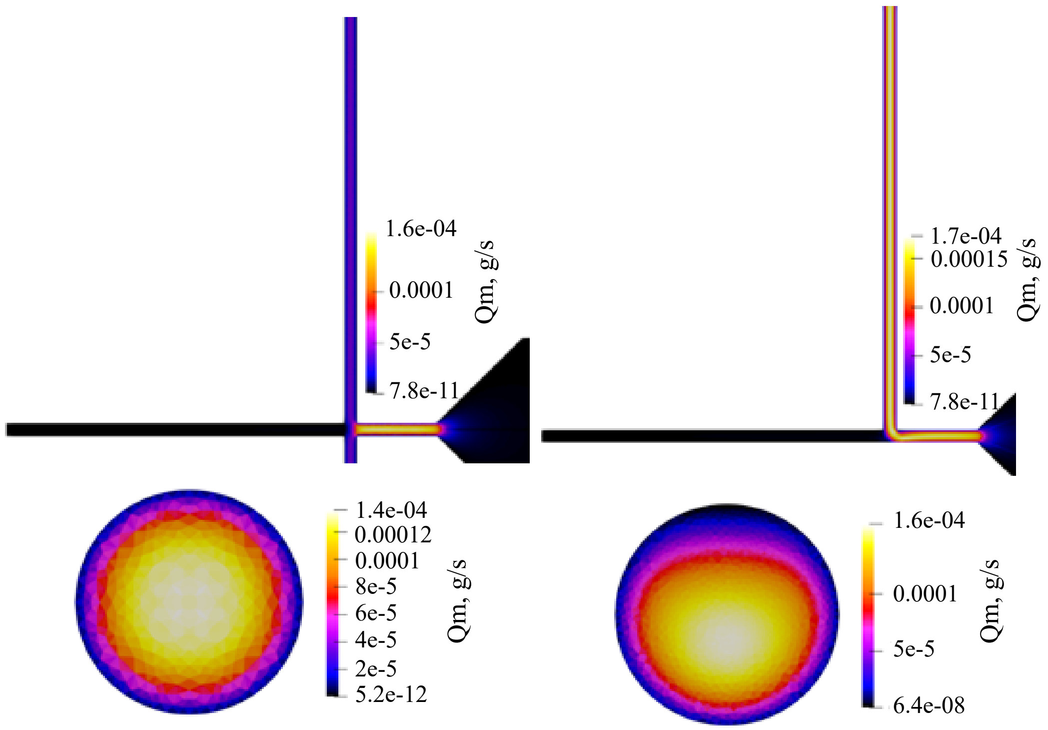


Fig. 6. Mass flow distribution in the cross-section of the capillary near the inlet of the feeding channel for eight and two feeding channels

**Discharge.** To form a plasma channel capable of efficiently guiding an accelerating laser pulse through it, an electrical discharge is applied to the cold gas flow. For modeling the discharge, we utilize the initial state of the gas obtained after establishing it during the filling stage.

The MHD model we employ does not include descriptions of the electrical breakdown stage. The breakdown lasts about 10 ns and minimally affects the properties of the plasma channel. For modeling the second stage, the gas is transitioned into a weakly ionized state by increasing the temperature to 0.3 eV. Fig. 7 and 8 demonstrate that this artificially induced initial temperature jump constitutes less than 5 % of the maximum discharge temperature and does not significantly impact the state of the electro-discharge plasma.

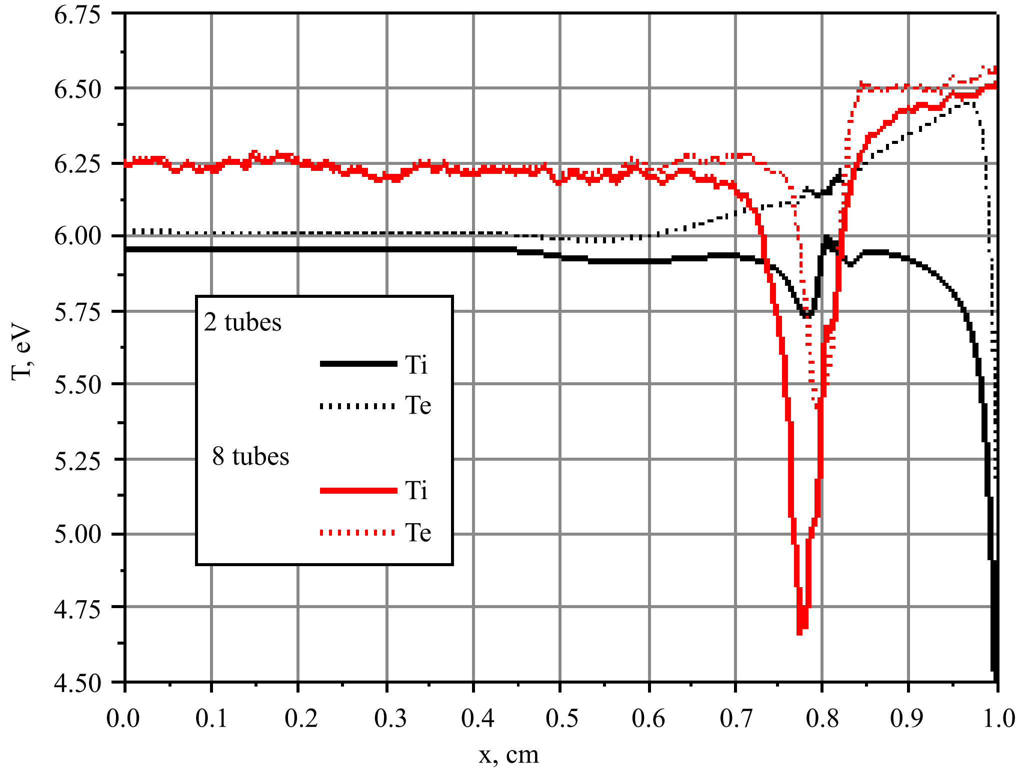


Fig. 7. Distribution of electron and ion temperature components along the axis of the capillary at the moment of maximum current for two and eight feeding channels

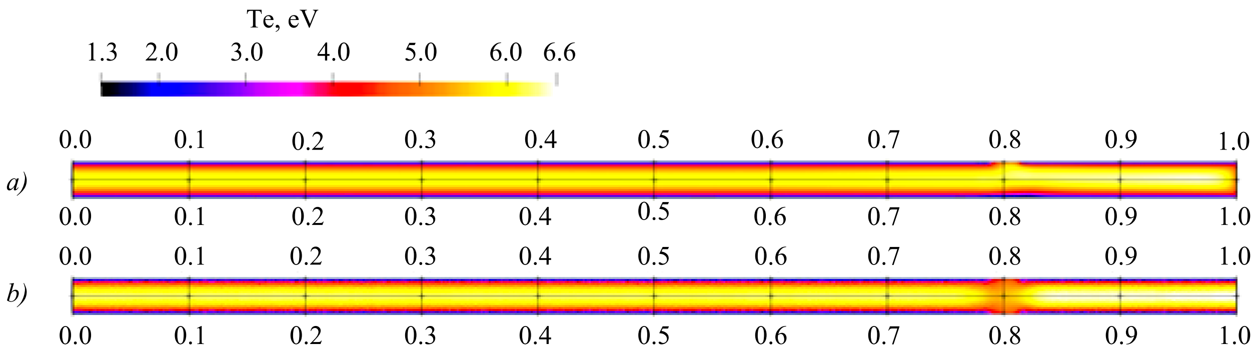


Fig. 8. Distribution of electron temperature in the longitudinal section at the moment of maximum current: *a* — 8 feeding channels; *b* — 2 feeding channels

The following distribution of electron density along the axis of the capillary for various time points has been obtained (Fig. 9). The slight increase in density near the exit during the initial period is due to the capillary gas experiencing some retardation as it displaces the gas that filled the nozzle towards the end of the first stage of the filling process.

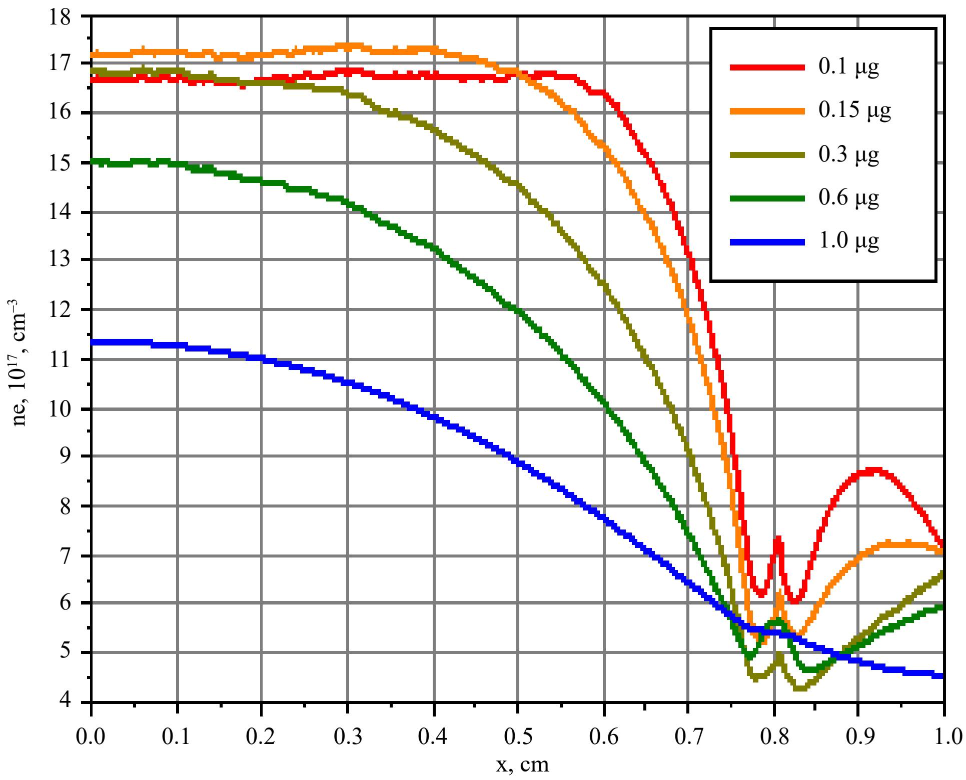


Fig. 9. Electron concentration along the axis of the capillary at different times relative to the start of the electrical discharge for a system with eight feeding channels

For cases with two and eight feeding channels, the distribution of plasma density during discharge is nearly identical with minor differences in the region from 0.75 to 1 cm (Fig. 10). This is caused by the displacement of discharge plasma into the feeding channels during the discharge process; it should be noted that the cross-sectional area through which gas enters the capillary is four times larger in the case of eight tubes compared to two tubes.

The most pronounced non-uniformity is observed in the flow section near the feeding channels, as shown in Fig. 11. In the junction area of the feeding channels, the electron density is approximately half that of the central part of the capillary. Additionally, good symmetry of distribution can be noted. It is reiterated that radial symmetry in the distribution and homogeneity of the channel along its axis are crucial for acceleration. The significant gradient of density along the boundaries of the forming waveguide also plays a crucial role in creating favorable conditions for the collimation of laser radiation in the waveguide, as clearly demonstrated in Figure 15.

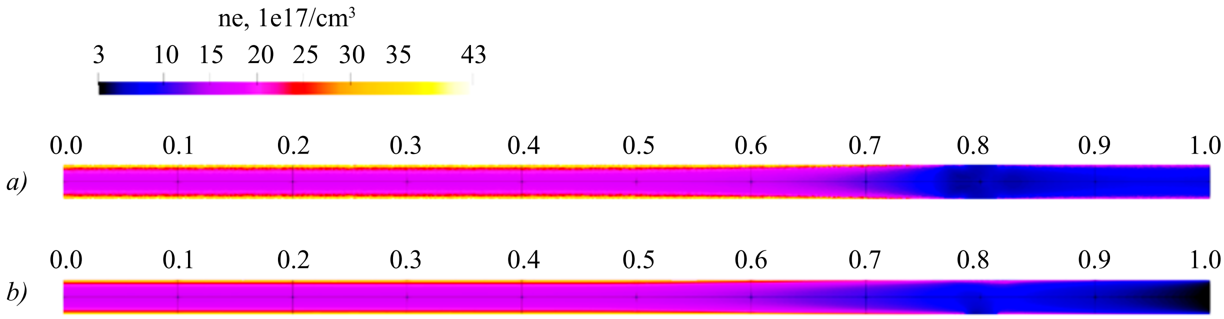


Fig. 10. Distribution of electron density in the longitudinal section at the moment of maximum current: *a* — 8 feeding channels; *b* — 2 feeding channels

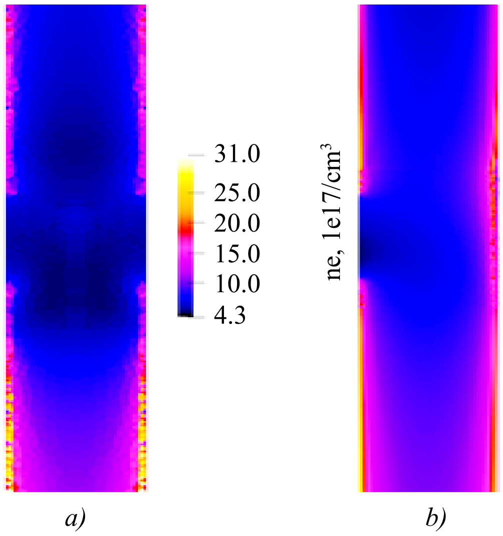


Fig. 11. Distribution of electron density in the longitudinal section near the attachment of feeding channels at the moment of maximum current: *a* — 8 feeding channels; *b* — 2 feeding channels

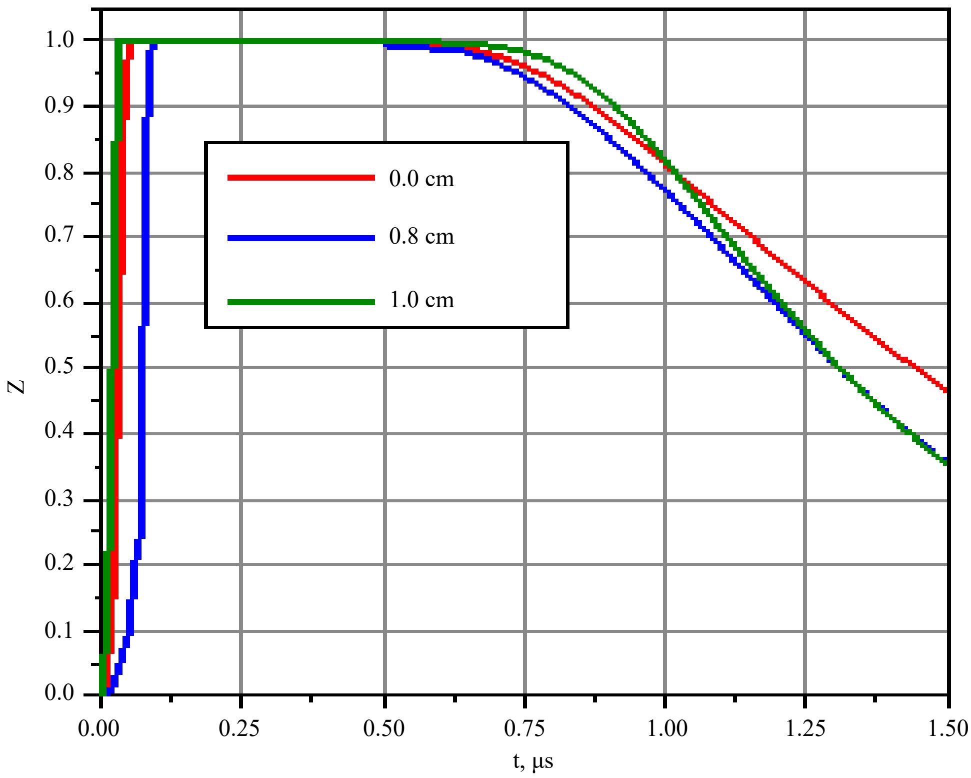


Fig. 12. Hydrogen ionization levels at three control points along the axis of the capillary (distance from the center indicated) as a function of time

The channel is considered prepared to pass an accelerating laser pulse through it when the hydrogen ionization level reaches unity. We examine the ionization evolution (Fig. 12) at three control points along the axis taken at specific distances from the capillary center: 0 cm — center of the main channel, 0.8 cm — point opposite the feeding channels, 1 cm — end of the capillary. Based on the data presented in Figure 12, it can be concluded that a waveguide with the required properties forms along the entire length of the capillary and exists from the moment of maximum current (150 ns) to approximately 700 ns, i. e., for a period of approximately 500–600 ns.

From the density distribution presented in Figure 10, it follows that there are differences in the plasma waveguide structures depending on the geometry of the feeding channels. This difference is insignificant for the electron density distribution in the central part of the capillary. Discrepancies in electron density distribution near the feeding channels and further towards the open end are much more pronounced — up to 50 % lower than the average density in the segment from 0.75 to 1 cm along the capillary length. In the case of eight feeding channels, a significant portion of the plasma is displaced into them, resulting in a region of reduced plasma density near the entrance of the feeding channels. In the case of two channels, plasma displacement into the channels is less noticeable, and plasma flows more through the ends of the capillary.

The most important characteristic of the plasma concerning its use as a working medium for electron acceleration by a laser pulse is the electron concentration along the axis of the capillary. The average electron concentration value at the moment of maximum current is nearly identical for both cases in the flow region between the central section of the capillary and up to a distance of approximately 0.75 cm from the center, with slight differences in the end regions, and is approximately $n_e \approx 1.8\times1018$ cm$^{-3}$. In the region of maximum rarefaction, from 0.75 to 1 cm, the electron concentration is approximately $n_e \approx 0.8\times1018$ cm$^{-3}$. It should be noted that these concentration values are in good agreement with the concentration value ~2×1018 cm$^{-3}$, determined in [2, 21] for a capillary with the same diameter and length as in the present work, calculated for an experiment with a laser pulse energy of ~3 J with a duration of about 30 fs.

Fig. 13 and 14 show the transverse distribution of density and electron concentration at the center of the tube (x = 0 cm). The obtained density values for eight and two feeding tubes are close to the values obtained in the two-dimensional variant. Minor differences in electron density distributions for the two capillary filling options are due to the different mesh structures used in these variants, which are also reflected in the temperature profile (Fig. 7, 8). Figure 15 presents the electron concentration distribution across the capillary at various distances from the center.

The transverse dynamics of capillary plasma, leading to the formation of a plasma channel suitable for laser acceleration, is analogous to that considered in [9], where calculations were based on a one-dimensional flow model under cylindrical symmetry approximation. Three-dimensional modeling shows that the lifetime of the plasma channel is determined by the plasma flow into the open ends of the capillary and partially backflow into the feeding channels.

The duration of the electrical pulse has less influence on the channel lifetime compared to a longer capillary — 10 centimeters or more.

Figures 16 and 17 show the distribution of electron concentration at the location of the attachment of feeding channels. In the case of eight channels, this area exhibits greater optical transparency compared to the two-channel variant. Apart from lower transparency, the "two-channel" system notably disrupts the radial symmetry of the plasma channel. The duration of the electrical discharge stage is measured from the moment of discharge initiation until nearly complete hydrogen recombination.

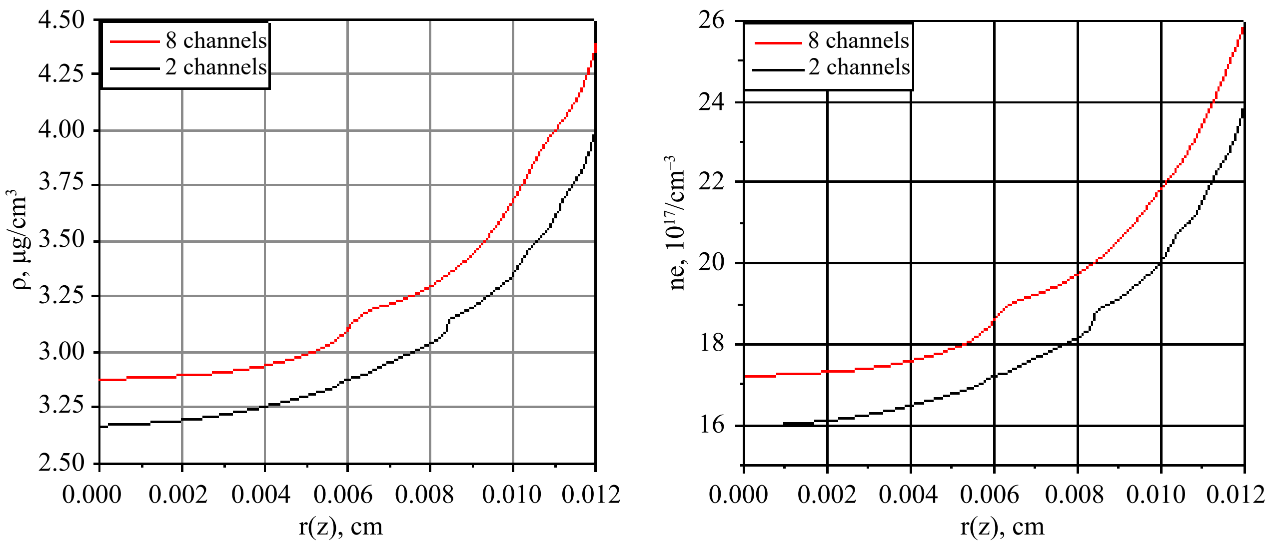


Fig. 13. Transverse distribution of electron density and concentration at the center of the capillary for two and eight feeding channels at the moment of maximum current

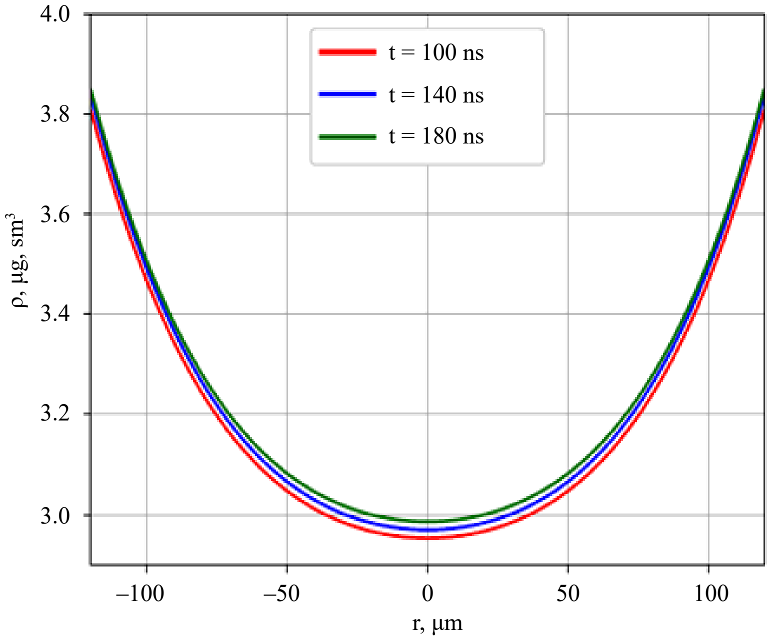


Fig. 14. Transverse distribution of electron density at the center of the capillary in the two-dimensional model [21]

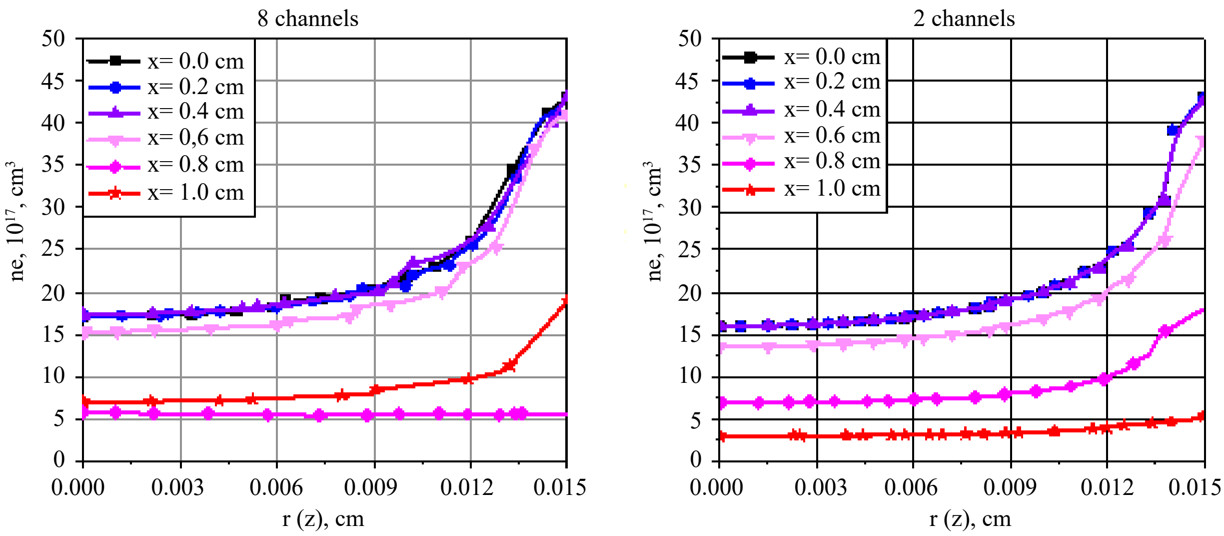


Fig. 15. Transverse distribution of electron concentration at various distances from the center of the capillary for eight and two feeding channels

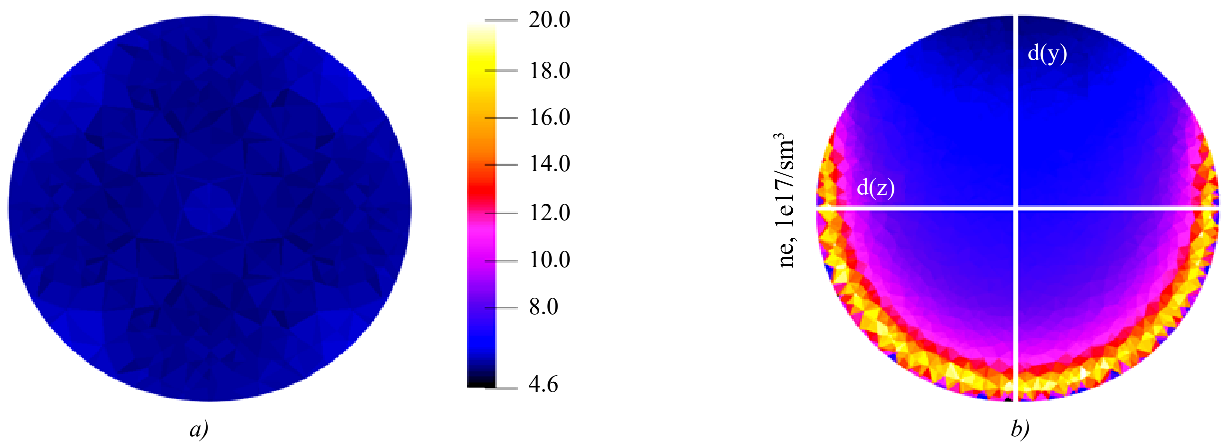


Fig. 16. Electron concentration distribution across the capillary section near the attachment of feeding channels ($x = 0.8$): *a* — 8 feeding channels; *b* — 2 feeding channels

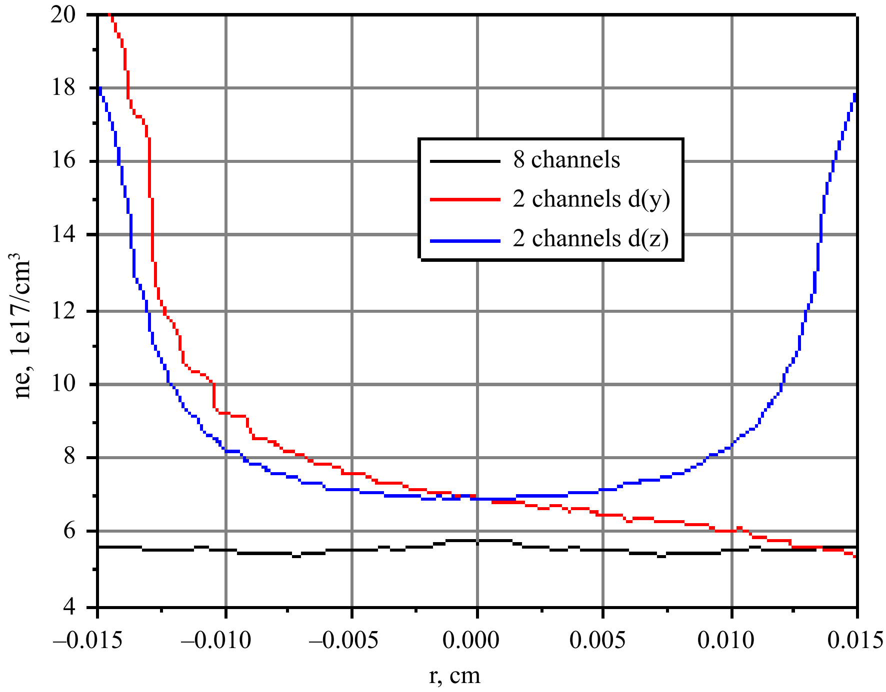


Fig. 17. Distribution of electron concentration across the diameter of the section in the case of eight feeding channels, as well as along the vertical and horizontal axes in the case of two feeding channels

**Gas Exhaustion and Capillary Refilling.** Upon completion of hydrogen recombination within the capillary, a sufficient amount of hot gas remains under high pressure. Active gas expansion continues towards the open ends and feeding channels, starting from the initiation of the electrical discharge.

Gas exhaustion is considered complete when the hydrogen pressure in the feeding reservoir exceeds that of the expanding gas, initiating the process of refilling the capillary with cold gas. It is noteworthy that during refilling, the central part of the capillary already contains gas which, as it cools down, returns to its initial state.

The refilling process occurs almost identically to the initial filling. The difference lies in a denser environment compared to its initial state, as well as a higher gas temperature within the “capillary + feeding channels” system. The times for initial and repeat fillings are found to be close; for the sake of analysis convenience, they are considered equal in the capillary operation cycles.

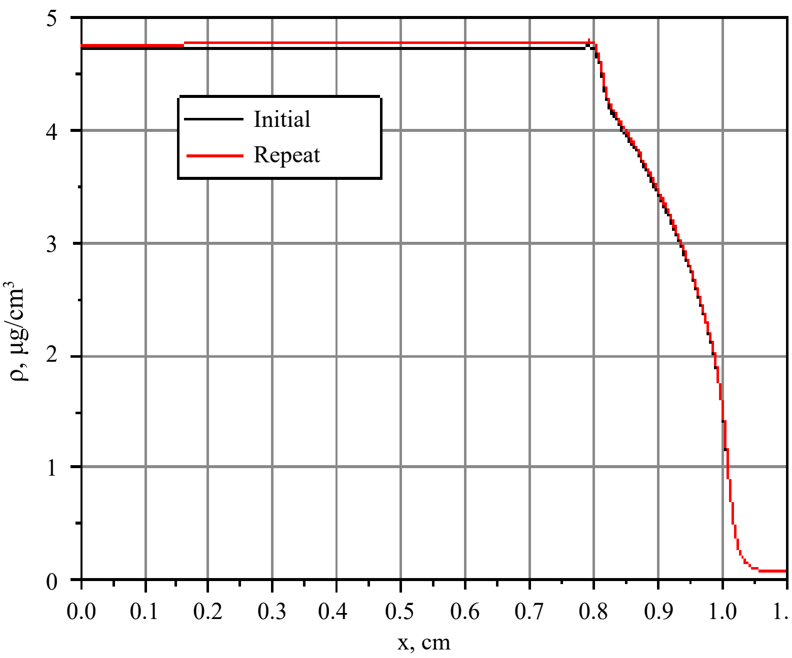


Fig. 18. Density profiles along the axis of the capillary for initial and repeat filling scenarios, illustrated for the case with two feeding channels

Fig. 18 shows a comparison of density profiles along the axis for initial and repeat filling for the case with two feeding channels.

**Discussion and Conclusion.** The calculated time for one cycle of "filling — discharge — relaxation" is presented in Table 1. In the calculation based on the two-dimensional model, the time for repeat filling does not exceed half of the time for initial filling.

Table 1

Calculated time for one cycle of "filling — discharge — relaxation"

| Mounting Type | 8 channels | 2 channels | 2D |
|---|---|---|---|
| Filling time, μs | 225 | 200 | 125 |
| Ionized state, μs | 5 | 5 | 5 |
| Release of heated gas, μs | < 50 | < 45 | |
| Total cycle time, μs | $\lesssim$280 | $\lesssim$250 | $\lesssim$130 (перв.)<br>$\lesssim$60 (повт.) |

The shape of the feeding channels (2 tubes, 8 tubes, two-dimensional filling model) has the greatest influence on the operating frequency of the short capillary. The diameters and lengths of the feeding channels evidently affect the filling rate. To a lesser extent, the temperature and pressure of the gas entering the system affect the cycle duration. The intensity of filling is determined by experimental conditions [2].

The mathematical model of the capillary system developed by the authors allows concluding that the capillary can operate in the frequency range from 1 to 16.5 kHz.

In conclusion, let's assess the energy gained by electrons during their acceleration by a laser pulse in the capillary discharge channel, for which we can use, for example, the formula proposed in [23]:

$$W\left(\text{GeV}\right) \sim \frac{0{,}4\,I\left(\text{W}/\text{cm}^2\right)}{n_e\left(1/\text{cm}^3\right)}, \tag{2}$$

where $W$ is the energy of accelerated electrons; $I \leq 10^{18}$ $W$/cm$^2$ is the intensity of the accelerator laser; $n_e$ is the average electron density along the path of the beam.

As initial data for estimation, we take the parameters of the plasma medium at the center of the capillary close to the maximum current strength (~150 ns). Using the data obtained during the discharge phase, we can expect electron energies during acceleration, according to formula (2), $W_e \leq 0.5$ GeV, which holds true for all three considered geometrical variants.

The obtained values of acceleration and potential operating frequency of the accelerator indicate the prospect of using a short-length capillary plasma accelerator. An important characteristic of the electron beam is its emittance. For a precise assessment, modeling based on a Particle-in-Cell approach, for example, in a ponderomotive approximation [5], is necessary. Corresponding computational experiments are the subject of further research.

**References**

1. Tajima T., Dawson J.M. Laser Electron Accelerator. *Phys. Rev. Lett.* 1979;43:267. https://doi.org/10.1103/PhysRevLett.43.267

2. Molodozhentsev A., Korn G., Maier A., Pribyl L. LWFA-driven Free Electron Laser for ELI-Beamlines. ICFA *Advanced Beam Dynamics Workshop on Future Light Sources*. JACoW, Geneva. 2018;60:62–67. https://doi.org/10.18429/JACoW-FLS2018-TUA2WC02

3. Leemans W., Esarey E. Laser-driven plasma-wave electron accelerators. *Phys. Today*. 2009;62(3):44.

4. Schroeder C.B., Esarey E., Geddes C.G.R., Benedetti C., Leemans W.P. Physics considerations for laser-plasma linear colliders. *Phys. Rev. Accel. Beams*. 2010;13:101301. https://doi.org/10.1103/PhysRevSTAB.13.101301

5. Leemans W.P., Gonsalves A.J., Mao H.-S., Nakamura K., Benedetti C., Schroeder C.B., et al. Multi-GeV Electron Beams from Capillary-Discharge-Guided Subpetawatt Laser Pulses in the Self-Trapping Regime. *Phys. Rev. Lett.* 2014;113:245002. https://doi.org/10.1103/PhysRevLett.113.245002

6. Gonsalves A.J., Nakamura K., Daniels J., Benedetti C., Pieronek C., de Raadt T.C.H., et al. Petawatt laser guiding and electron beam acceleration to 8 GeV in a laser-heated capillary discharge waveguide. *Phys. Rev. Lett.* 2019;122:084801. https://doi.org/10.1103/PhysRevLett.122.084801

7. Esarey E., Schroeder C.B., Leemans W.P. Physics of laser-driven plasma-based electron accelerators. *Rev. Mod. Phys.* 2009;81:1229. https://doi.org/10.1103/RevModPhys.81.1229

8. Spence D.J., Hooker S.M. Investigation of a hydrogen plasma waveguide. *Phys. Rev. E.* 2001;63:015401(R). https://doi.org/10.1103/PhysRevE.63.015401

9. Bobrova N.A., Esaulov A.A., Sakai J.-I., Sasorov P.V., Spence D.J., Butler A., et al. Simulations of a hydrogen-filled capillary discharge waveguide. *Phys. Rev. E.* 2002;65:016407. https://doi.org/10.1103/PhysRevE.65.016407

10. Hosokai T., Kando M., Dewa H., Kotaki H., Kondo S., Hasegawa N., et al. Optical guidance of terrawatt laser pulses by the implosion phase of a fast z-pinch discharge in a gas-filled capillary. *Opt. Lett.* 2000;25:10–12. https://doi.org/10.1364/OL.25.000010

11. Kameshima T., Kotaki H., Kando M., Daito I., Kawase K., Fukuda Y., et al. Laser pulse guiding and electron acceleration in the ablative capillary discharge plasma. *Phys. Plasmas*. 2009;16:093101. https://doi.org/10.1063/1.3212589

12. Gonsalves A.J., Nakamura K., Lin C., Panasenko D., Shiraishi S., Sokollik T, et al. Tunable laser plasma accelerator based on longitudinal density tailoring. *Nat. Phys*. 2011;7:862–866. https://doi.org/10.1038/nphys2071

13. Pieronek C., Gonsalves A., Benedetti C., Bulanov S., van Tilborg J., Bin J., et al. Laser-heated capillary discharge waveguides as tunable structures for laser-plasma acceleration. *Phys. Plasmas*. 2020;27:093101. https://doi.org/10.1063/5.0014961

14. Bobrova N.A., Sasorov P.V., Benedetti C., Bulanov S.S., Geddes C.G.R., Schroeder C.B., et al. Laser-heater assisted plasma channel formationin capillary discharge waveguides. *Phys. Plasmas*. 2013;20:020703. https://doi.org/10.1063/1.4793447

15. Bagdasarov G.A., Bobrova N.A., Olkhovskaya O.G., Gasilov V.A., Benedetti C., Bulanov S.S., et al. Creation of axially uniform plasma channelin laser-assisted capillary discharge. *Phys. Plasmas*. 2021;28:053104. https://doi.org/10.1063/5.0046428

16. Gonsalves A.J., Liu F., Bobrova N.A., Sasorov P.V., Pieronek C., Daniels J, et al. Demonstration of a High Repetition Rate Capillary Discharge Waveguide. *J. Appl. Phys.* 2016;119:033302. https://doi.org/10.1063/1.4940121

17. Alejo A., Cowley J., Picksley A., Walczak R., Hooker S.M. Demonstration of kilohertz operation of hydrodynamic optical-field-ionized plasma channels. *Phys. Rev. Accel. Beams.* 2022;25:011301. https://doi.org/10.1103/PhysRevAccelBeams.25.011301

18. D'Arcy R., Chappell J., Beinortaite J., Diederichs S., Boyle G., Foster B., et al. Recovery time of a plasma-wakefield accelerator. *Nature*. 2022;603:58–62. https://doi.org/10.1038/s41586-021-04348-8

19. Bagdasarov G.A., Kruchinin K.O., Molodozhentsev A.Yu., Sasorov P.V., Bulanov S.V., Gasilov V.A. Discharge Plasma Formation in Square Capillary with Gas Supply Channels. *Phys. Rev. Res.* 2022;4:013063. https://doi.org/10.1103/PhysRevResearch.4.013063

20. Gasilov V.A., Boldarev A.S., Olkhovskaya O.G., Boykov D.S., Sharova Yu.S., Savenko N.O, et al. MARPLE: software for multiphysics modelling in continuous media. *Numerical Methods and Programming*. 2023;24(4):316–338. https://doi.org/10.26089/NumMet.v24r423

21. Sasorov P., Bagdasarov G., Bobrova N., Grittani G., Molodozhentsev A., Bulanov S.V. Capillary discharge in the high repetition rate regime. *Physical Review Research*. 2024;6:013290. https://doi.org/10.1103/PhysRevResearch.6.013290

22. Savenko N.O. On the difference approximation of gasdynamic flows on the free boundary of the computational domain. *Preprints of the Institute of Applied Mathematics named after M.V. Keldysh*. 2023;51:28. (in Russ.). https://doi.org/10.20948/prepr-2023-51

23. Leemans W.P., Nagler B., Gonsalves A.J., Toth Cs., Nakamura K., Geddes C.G.R., et al. GeV electron beams from a centimeter-scale accelerator. *Nature physics*. 2006;2:696–699. https://doi.org/10.1063/1.2718524

24. Braginsky S.I., Leontovich M.A. (eds). Phenomena of transport in plasma. In: *Questions of plasma theory*. Issue 1. GosAtomIzdat. 1963. P. 183–272. (in Russ.).

**Received** 04.06.2024
**Revised** 24.06.2024
**Accepted** 25.06.2024

*About the Authors:*

**Vladimir A. Gasilov,** Principal Researcher, Keldysh Institute of Applied Mathematics of Russian Academy of Sciences (4, Miusskaya sq., Moscow, 125047, RF), ORCID, MathNet, vgasilov@keldysh.ru

**Nikita O. Savenko,** Junior Researcher, Keldysh Institute of Applied Mathematics of Russian Academy of Sciences (4, Miusskaya sq., Moscow, 125047, RF), ORCID, MathNet, savenkonkt@gmail.com

**Yulia S. Sharova,** Junior Researcher, Keldysh Institute of Applied Mathematics of Russian Academy of Sciences (4, Miusskaya sq., Moscow, 125047, RF), ORCID, MathNet, yulia-shar@mail.ru

*Claimed contributor-ship:*
All authors have made an equivalent contribution to the preparation of the publication.

*Conflict of interest statement*
The authors do not have any conflict of interest.

*All authors have read and approved the final manuscript.*

**Поступила в редакцию** 04.06.2024
**Поступила после рецензирования** 24.06.2024
**Принята к публикации** 25.06.2024

*Об авторах:*

**Гасилов Владимир Анатольевич,** главный научный сотрудник, Институт прикладной математики им. М.В. Келдыша Российской академии наук (РФ, 125047, Москва, Миусская пл., 4), ORCID, MathNet, vgasilov@keldysh.ru

**Савенко Никита Олегович,** младший научный сотрудник, Институт прикладной математики им. М.В. Келдыша Российской академии наук (РФ, 125047, Москва, Миусская пл., 4), ORCID, MathNet, savenkonkt@gmail.com

**Шарова Юлия Сергеевна,** младший научный сотрудник, Институт прикладной математики им. М.В. Келдыша Российской академии наук (РФ, 125047, Москва, Миусская пл., 4), ORCID, MathNet, yulia-shar@mail.ru

*Заявленный вклад соавторов:*

Все авторы сделали эквивалентный вклад в подготовку публикации.

*Конфликт интересов*

Авторы заявляют об отсутствии конфликта интересов.

*Все авторы прочитали и одобрили окончательный вариант рукописи.*